



Evaluating the durability and performance of polyoxometalate-ionic liquid coatings on calcareous stones: Preventing biocolonisation in outdoor environments

Stéphanie Eyssautier-Chuine, Isabel Franco-Castillo, Archismita Misra, Julien Hubert, Nathalie Vaillant-Gaveau, Carsten Streb, Scott Mitchell

► To cite this version:

Stéphanie Eyssautier-Chuine, Isabel Franco-Castillo, Archismita Misra, Julien Hubert, Nathalie Vaillant-Gaveau, et al.. Evaluating the durability and performance of polyoxometalate-ionic liquid coatings on calcareous stones: Preventing biocolonisation in outdoor environments. Science of the Total Environment, 2023, 884, pp.163739. 10.1016/j.scitotenv.2023.163739 . hal-04088249

HAL Id: hal-04088249

<https://hal.univ-reims.fr/hal-04088249>

Submitted on 12 May 2023

HAL is a multi-disciplinary open access archive for the deposit and dissemination of scientific research documents, whether they are published or not. The documents may come from teaching and research institutions in France or abroad, or from public or private research centers.

L'archive ouverte pluridisciplinaire **HAL**, est destinée au dépôt et à la diffusion de documents scientifiques de niveau recherche, publiés ou non, émanant des établissements d'enseignement et de recherche français ou étrangers, des laboratoires publics ou privés.



Evaluating the durability and performance of polyoxometalate-ionic liquid coatings on calcareous stones: Preventing biocolonisation in outdoor environments

Stéphanie Eyssautier-Chuine ^{a,*}, Isabel Franco-Castillo ^{b,c}, Archismita Misra ^d, Julien Hubert ^a, Nathalie Vaillant-Gaveau ^e, Carsten Streb ^{d,f}, Scott G. Mitchell ^{b,c,**}

^a Groupe d'Étude sur les Géomatériaux et les Environnements Naturels Anthropiques et Archéologiques 3795 (GEGENAA) - SFR Condorcet FR CNRS 3417 – 2, Esplanade Roland Garros, Université de Reims Champagne-Ardenne, 51100 cedex Reims, France

^b Instituto de Nanociencia y Materiales de Aragón (INMA-CSIC/UNIZAR), Consejo Superior de Investigaciones Científicas-Universidad de Zaragoza, c/ Pedro Cerbuna 12, 50009 Zaragoza, Spain

^c CIBER de Bioingeniería, Biomateriales y Nanomedicina, Instituto de Salud Carlos III, 28029 Madrid, Spain

^d Institute of Inorganic Chemistry I, Ulm University, Albert-Einstein-Allee 11, 89081 Ulm, Germany

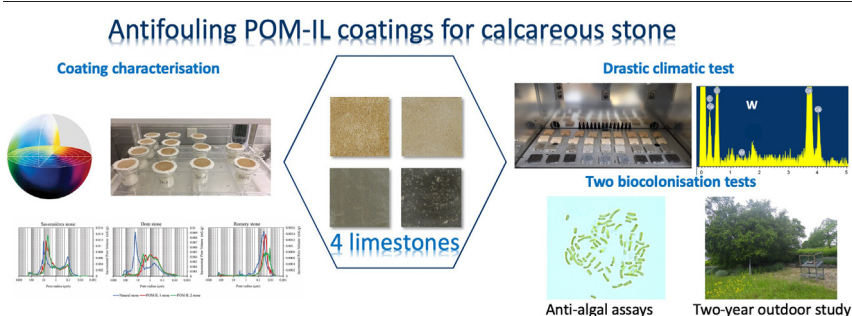
^e Unité de Recherche EA 4707 Résistance Induite et Bioprotection des Plantes (RIBP), SFR Condorcet FR CNRS 3417, UFR Sciences Exactes et Naturelles, Université de Reims Champagne-Ardenne, Reims, France

^f Department of Chemistry, Johannes Gutenberg University Mainz, Duesbergweg 10-14, 55128 Mainz, Germany

HIGHLIGHTS

- POM-IL coatings did not significantly alter the total porosity of calcareous stones.
- Macropore size variation for Dom and Savonnières did not alter water vapour transfer.
- Weathered POM-IL coatings prevented colonisation of stones by green algae.
- Biocidal POM-ILs have the potential to prevent biocolonisation in outdoor environments.

GRAPHICAL ABSTRACT



ARTICLE INFO

Guest Editor: Patricia Sanmartín

Keywords:

Polyoxometalate-ionic liquid (POM-IL)
Biocide durability
Calcareous stone
Biocolonisation mitigation
Water vapour permeability

ABSTRACT

Rock-based materials exposed to outdoor environments are naturally colonised by an array of microorganisms, which can cause dissolution and fracturing of the natural stone. Biocolonisation of monuments and architectures of important cultural heritage therefore represents an expensive and recurring problem for local authorities and private owners alike. In this area, preventive strategies to mitigate biocolonisation are generally preferred to curative approaches, such as mechanical cleaning by brush or high-pressure cleaning, to remove pre-existing patina. The aim of this work was to study the interaction between biocidal polyoxometalate-ionic liquid (POM-IL) coatings and calcareous stones and evaluate the capacity of these coatings to prevent biocolonisation through a series of accelerated ageing studies in climate chambers, carried out in parallel with a two-year period of outdoor exposure in north-eastern France. Our experiments show that POM-IL coatings did not affect water vapour transfer nor significantly alter the total porosity of the calcareous stones. Simulated weathering studies replicating harsh (hot and wet) climatic weather conditions demonstrated that the colour variation of POM-IL-coated stones did not vary significantly with respect to the natural uncoated stones. Accelerated biocolonisation studies performed on the weathered POM-IL-coated stones proved that the coatings were still capable of preventing colonisation by an algal biofilm. However, a combination of colour measurements, chlorophyll fluorescence data, and scanning electron microscopy imaging of stones aged outdoors in

* Corresponding author.

** Correspondence to: S.G. Mitchell, Instituto de Nanociencia y Materiales de Aragón (INMA-CSIC/UNIZAR), Consejo Superior de Investigaciones Científicas-Universidad de Zaragoza, c/ Pedro Cerbuna 12, 50009 Zaragoza, Spain.

E-mail addresses: stephanie.eyssautier@univ-reims.fr (S. Eyssautier-Chuine), scott.mitchell@csic.es (S.G. Mitchell).

northern France for two years showed that coated and uncoated stone samples showed signs of colonisation by fungal mycelium and phototrophs. Altogether, our results demonstrate that POM-ILs are suitable as preventative biocidal coatings for calcareous stones, but the correct concentrations must be chosen to achieve a balance between porosity of the stone, the resulting colour variation and the desired duration of the biocidal effect over longer periods of time, particularly in outdoor environments.

1. Introduction

Many rock-based materials exposed to the outdoor environment are naturally colonised by microorganisms. The deteriorative effects related to biocolonisation, and possible shifts between neutral or even bioprotective behaviour and biodeterioration actions, depend on several factors related to climate, micro-environment, pre-existing weathering of the substrates, nature of the substrates, etc. A vast corpus of scientific research has explored such issues in recent years (Alisi, 2011; Bartoli et al., 2014; Urzì et al., 2014; Warscheid and Braams, 2000). Biofilms growing on monuments and statues are defined as a microbial community attached to a solid surface and are composed of phototrophic microorganisms as pioneering colonisers like microalgae, cyanobacteria, lichens which synthesise organic extracellular organic matter, and facilitate the growth of heterotrophic microorganisms such as bacteria and fungi (Di Martino, 2016; Pinna, 2021; Romani et al., 2021; Santo et al., 2021). Biofilm growth on buildings which was previously regarded in romantic and bucolic terms is now generally considered as a threat to be mitigated in order to preserve and protect built cultural heritage (Warscheid and Leisen, 2011). Nowadays, the biological colonisation of monuments is a relevant and an expensive problem for local authorities, museums, and private collectors who strive against an everlasting phenomenon. Two main strategies against biocolonisation are often undertaken, the first is a curative approach (to remove existing biofilms) which consists of a mechanical - physical - cleaning of the biological patina by brush, UV irradiation, thermal treatment, laser (Bertuzzi et al., 2017; Mascalchi et al., 2020; Pfendler et al., 2018; Vlasov et al., 2019), followed by the application of biocides that are active against a broad range of microorganisms (Coutinho et al., 2016; Favero-Longo et al., 2017; Speranza et al., 2012). The second strategy is a preventive approach (to delay biocolonisation and subsequent cleaning operations) to achieve a longer lasting protection of stone heritage. Further mitigation strategies included the control of external factors like limiting the water content inside the stones by optimising the rain draining and favouring sunlight areas which help to a faster rain evaporation (Liu et al., 2020). Nevertheless, limited control over external factors means that a preventive application with biocidal products is routinely used to achieve a longer-lasting action against a microbial colonisation. Importantly, the use of biocides on heritage involves important requirements, such as product efficacy and transparency (colourless coatings), substrate/surface compatibility, as well as the potential to re-treat/re-apply the coating to achieve the desired long-term efficacy. Nanomaterials are considered as innovative alternatives to conventional biocides based on quaternary ammonium compounds and have been successfully applied in various fields where disinfection is required, such as water purification, food safety, preventing infection and disease, and are widespread in heritage conservation. The large range of metal and metal-oxide nanoparticles and carbon nanomaterials currently known have enhanced their use in heritage conservation applications as consolidants, water repellents and biocides (Becerra et al., 2020; Carrapiço et al., 2023; Gómez-Ortiz et al., 2014; Shilova et al., 2022; Zarzuela et al., 2016). For example, there has been significant in the application of TiO₂-based materials based on their self-cleaning and antimicrobial properties (Colangiuli et al., 2019; La Russa et al., 2014; Luvidi et al., 2016; Ruffolo et al., 2017; Shilova et al., 2020). However, recently ionic liquids (ILs) have gained attention as a new generation of multifunctional materials for the Cultural Heritage field (De Leo et al., 2021; Franco-Castillo et al., 2021; Lo Schiavo et al., 2020; Romani et al., 2022). The use of stable water insoluble ionic

liquid coatings that prevent biofilm formation have the potential to generate a lower environmental impact than nanoparticles whose the ecotoxicological impact arise from their release through aqueous lixiviation into the environment (Brunelli et al., 2021; Reyes-Estebanez et al., 2018).

For the last two decades, ionic liquids have drawn a lot of academic interest owing to their unique physicochemical properties like low melting point, high viscosity, low vapour pressure, molecular-level tunability, and low environmental impact (Jordan and Gathergood, 2015; Petkovic et al., 2011). Traditionally, ILs are formed by combining bulky organic cations such as alkylpyridinium or imidazolium with organic or inorganic anions such as Cl⁻, BF₄⁻ or PF₆⁻, giving ILs which are typically liquid at room temperature, have negligible vapour pressure and offer a wide range of useful applications in synthesis, catalysis and electrochemistry (Hallett and Welton, 2011; Smarsly and Kaper, 2005; Wasserscheid and Keim, 2000). When the classical IL anions are exchanged for polyoxometalate anions, polyoxometalate-ionic liquids (POM-ILs) are obtained (Herrmann et al., 2014b). Polyoxometalates (POMs) are a diverse class of nanoscale molecular metal oxides, which are characterised by a wide and versatile range of physicochemical properties that can be tuned on the molecular level (Cronin and Müller, 2012). Their redox properties and high oxidation activity also make them useful to a wide variety of applications, from catalysis (Streb, 2012) to medicine (Daima et al., 2014) while importantly POMs also display antimicrobial activity (Bijelic et al., 2018). POM-ILs have been employed as functional composites for universal pollutant removal (Herrmann et al., 2017) or reactive surface protecting anti-corrosion coatings (Herrmann et al., 2014a; Misra et al., 2018) because the composites can be tailored to target biological, organic and inorganic pollutants including microbes, acids and reactive oxygen species (Kubo et al., 2017). Rheological properties and hydrophobicity can be tuned by chemical design which is important to obtain surface coatings.

Our research has focused on the design and development of multifunctional POM-ILs as hydrophobic acid-stable coatings with antimicrobial and anticorrosive properties to prevent biocolonisation of natural carbonate stones (Franco-Castillo et al., 2022; Misra et al., 2018; Rajkowska et al., 2020). Proof-of-principle studies demonstrated how long-chain quaternary alkylammonium cations combined with acid-stable polyoxotungstate anions can be used to access room-temperature POM-ILs which combine facile application and high surface adhesion on porous and non-porous stone surfaces with high surface hydrophobicity, acid stability, and biocidal features (Misra et al., 2018). Remarkably enhanced corrosion-resistance was achieved under harsh chemical and mechanical conditions. The stone samples were even exposed to model bacterial strains (Gram negative *E. coli* and Gram positive *B. subtilis*) in order to establish the effective resistance of the POM-ILs against microbial growth. In general, both bacterial strains incubated with POM-ILs showed evidence of stress and damage including general loss of cell shape, cell membrane damage and leakage of cytoplasmic material. POM-IL coated stones prevented bacterial biofilm formation. Furthermore, we have demonstrated that POM-IL can be deployed as innovative protective coatings against lampenflora (green cyanobacteria and algae) growing on the bas-reliefs carved in the underground Pommery Champagne Cellar in Reims, France (Franco-Castillo et al., 2022). Biocidal assays carried out in laboratory demonstrated how two different colourless POM-IL coatings were more effective than the commercial Preventol RI80 against two algal strains isolated from the Pommery bas reliefs, *Pseudostichococcus monallantoides* and *Chromochloris zofingiensis*.

We have established that water-insoluble, high-viscosity POM-ILs can be deployed as effective biocidal coatings in the laboratory against a broad spectrum of microbes, including bacteria and cyanobacteria, moulds, and algae. However, their activity in simulated and real outdoor environments has yet to be investigated. Here we report on the durability and performance of biocidal POM-IL treatments coated on four limestones widely used in buildings and monuments through a series of accelerated, drastic weathering studies in climate chambers and algal biocolonisation studies, carried out in parallel with a two-year period of outdoor exposure in north-eastern France. The investigation is based on colorimetric measurements and chlorophyll fluorescence data. Porosimetric studies and water vapour permeability tests have been conducted on selected stones and complementary SEM-EDX analyses have been conducted to qualitatively assess the durability of the treatments and efficacy upon weathering.

2. Material and methods

2.1. Presentation of the stones

Four model calcareous stones were selected for their wide use in buildings and monuments in North-East France and Belgium and for their different visual aspects, intrinsic properties, susceptibility to weathering. Dom Stone (DO) (Bajocian, 180 My) is a russet macroporous limestone with 21.4 % of well-connected porosity (Eyssautier-Chuine et al., 2018). It is composed of bioclastic debris (50 %) surrounded in a calcitic cement. Savonnières stone (SA) (Lower Tithonian, 150 My) is a clear grain-supported facies with large elements (Eyssautier-Chuine et al., 2021). It is a macroporous stone highly connected with a porosity of 34.9 %. SA has been employed to build monuments and is now a restoration stone. Both porous stones are employed as ashlar for walls, door, and window frames and for sculptures. They are altered by the rainfall and wind driving to an alveolization, and they are strongly sensitive to the biological colonisation leading to scaling of the substrate. Romery stone (RO) (Sinemurian, 195 My) is a grey sandy limestone with a low porosity (4.8 %) and capillarity. It is employed in walls and pavements and its low porosity does not avoid the biocolonisation due to its roughness. Finally, the Belgian Blue Stone® (BB) (Tournaisian, 350 My) has been used to build many monuments, buildings (e.g., door and window frames), pavements and graves in Belgium. BB is a dark compacted limestone made of sea fossils like corals, shells and crinoids surrounded by a fine dark grey mud. The porosity is low from 0.03 % up to 1 % measured in Hg porosimetry and reported at 0.28 % (Pereira et al., 2015), however, BB is known to be susceptible to biocolonization depending on the exposure and orientation conditions, e.g., the stagnation of water at a horizontal BB stone surface such as graves.

2.2. POM-IL biocides

POM-ILs 1 and 2 were synthesised according to a previously reported synthetic procedure (Misra et al., 2018). Both POM-ILs are based on the same lacunary Keggin polyoxoanion ($[\alpha\text{-SiW}_{11}\text{O}_{39}]^{8-}$), whose negative charge is balanced by a tetraalkylammonium cation: tetraheptylammonium (POM-IL1) and trihexyltetradecylammonium (POM-IL2). POM-ILs were applied as biocidal treatments to prevent the proliferation of microorganisms. POM-ILs were dissolved in acetone and applied at a concentration of 100 mg/mL, on the top face of three non-colonised stone slabs ($1 \times 5 \times 5$ cm in dimension) for each treatment and each test, and of four stone discs (5×0.5 cm in dimension) per treatment for the water vapour permeability test, and on all faces of three cubes ($0.5 \times 0.5 \times 1$ cm dimension) per treatment for Hg porosimetry. Weight measurements indicated that non-porous stones BB & RO, the coverage was ca. 0.5 mg/cm^2 for slabs and discs (60 mg/cm^3 for cubes), while for porous stones DO & SA the coverage was closer to 1 mg/cm^2 (300 mg/cm^3 for cubes). The employed concentration of the treatments was already tested in two accelerated biocolonisation tests on chalk stone (Franco-Castillo et al., 2022) and

on DO, SA and RO stones in a preliminary test with coated stones which were not previously aged like in this study (Fig. S1).

2.3. Evaluation of surface changes upon treatment and treatment durability

2.3.1. Colourimetry

The colour of stone samples was measured by using a Chroma Meter CR-400 from Konica-Minolta with a light projection tube CR-A33c of 11 mm diameter (corresponding to the measurement zone). Calibrations were performed with a white ceramic plate CR-A43. Values are given in the CIELAB colour space (European Committee for Standardization, 2011). Three parameters determine the colour location in colour space: L^* indicates lightness (0 = absolute black, 100 = absolute white), and a^* and b^* are the chromaticity coordinates. a^* is the position between green ($a^* < 0$) and red ($a^* > 0$); b^* is the position between blue ($b^* < 0$) and yellow ($b^* > 0$).

The CIELAB lightness and chroma differences were calculated: ΔL^* , Δa^* , Δb^* correspond to the differences between different surface conditions: coated and no coated stones, before and after the climatic test, the biological colonisation of stones through time (accelerated and outdoor biocolonisation tests). The global colour variation (ΔE^*_{ab}) was calculated as follows:

$$\Delta E^*_{ab} = \sqrt{\Delta L^{*2} + \Delta a^{*2} + \Delta b^{*2}}$$

Colour measurements were carried out on the upper surface of the slabs by taking 30 measurements per sample to assess the stone aspect before and after coating. Then the colour change was surveyed by 20 measurements per sample before and after the simulated climatic test, after the inoculation of algae (T0) for the accelerated biocolonisation test then every week (for five weeks) and every two months for the outdoor biocolonisation test (for two years). In this last test, every sample surface was wet before measurements because the wetness of stones changed according to the weather, the season, the time of the measurements that could make an artefact by a darkening of stones which was not assigned to the biocolonisation. Finally, an average of the colour parameters was established for each type of stone.

2.3.2. Water vapour permeability

The water vapour permeability investigates the diffusion of water vapour through stone and was performed for high porous stones (Dom and Savonnières), on four uncoated (control) and four coated stones. The European Standard for cultural heritage (European Committee for Standardization, 2010) details its measurement on stone discs 50 mm in diameter and 5 mm thick that we especially cut for this experiment. Discs were sealed in a glass cup containing water and placed in a desiccator (relative humidity maintained at ca. 53 % using a saturated solution of magnesium nitrate; temperature maintained at 20 ± 2 °C). The apparatus of disc in glass cup are weighted before and every 24 h until stabilisation of the weight. The water vapour permeability (δp) was calculated with the following formula and the average was computed from the measurements of control and coated stones:

$$\delta p = \frac{G}{A \cdot \Delta p_v} \cdot D \text{ (kg} \cdot \text{m}^{-1} \cdot \text{s}^{-1} \cdot \text{Pa}^{-1})$$

with $G = \frac{\Delta m}{\Delta t}$ ($\text{kg} \cdot \text{s}^{-1}$): the slope of the linear part of the curve corresponding to the mass variation in function of the time

A : surface of the disc (m^2)

Δp_v : variation of water vapour pressure on both sides of the cup (Pa)

D : thickness of the disc (m)

2.3.3. Porosity and pore access radii

Dom, Savonnières and Romery porous networks were investigated with triplicates of $1 \times 0.5 \times 0.5$ cm dimension, and they were coated on every face. Data were obtained with a mercury intrusion porosimeter

(Micromeritics Autopore IV 9500), reaching a pressure of 247 MPa and measuring pore radii sizes from 0.003 to 178 μm . The BB network was also investigated but the porosity was so weak that the porous network of this stone was below the limit of detection of the technique. In consequence, the impact of coatings on the BB porous network could not be investigated.

2.3.4. Chlorophyll *a* fluorescence (*chlF*)

Ten measurements were carried out directly on each slab with a Junior PAM Chlorophyll Fluorometer (Walz, Effeltrich, Germany) (Eyssautier-Chuine et al., 2021). This device detects and quantifies the chlorophyll *a* fluorescence emitted by plants and microalgae, it was connected to the sample with a flexible 1 mm active diameter fibre optic that employed a visible blue power LED (460 nm) for pulse modulated and saturating pulses. It was used with the pulse-amplitude modulated (PAM) in combination with saturating pulse analysis of fluorescence quenching. This technique was carried out every week during the accelerated biocolonisation test, where all stones are wet because of the regular intake of medium in each cup, and every two months during the outdoor biocolonisation test, where all stone surfaces were wet before measurements like in colorimetry. The initial fluorescence (F_0) was obtained after 30 min of dark adaptation. Maximal fluorescence (F_M) was obtained with a saturating flash (1 s, PAR:7000 $\mu\text{mol}\cdot\text{m}^{-2}\cdot\text{s}^{-1}$, Blue LED at 445 nm). The ratio of variable to maximal fluorescence (maximum quantum yield of PSII) was calculated as $F_V/F_M = (F_M - F_0)/F_M$.

2.3.5. Scanning Electron Microscopy (SEM)

Scanning Electron Microscopy (SEM) images and energy dispersive X-ray spectroscopy (EDX) spectra were acquired using a field emission SEM Inspect F50 with an EDX system INCA PentaFETx3 (FEI Company, Eindhoven, The Netherlands). The observations were carried out on stones after the outdoor test with the aim of detecting the development of any biological patina on stones. Samples were previously sawn dry to not alter the surface, with a diamond saw to get $1 \times 1 \times 0.5$ cm dimension. Samples were coated with carbon prior to SEM imaging.

2.4. Experimental design

2.4.1. Simulated weathering test

Simulated weathering, combined with the accelerated biocolonisation tests (see Section 2.4.2., below), aims to investigate the experimental treatments' residual efficacy when subjected to particularly harsh exposure conditions. These can be considered representative of possible climate change-related future scenarios in the geographical areas where the tested stones are traditionally employed. The simulated weathering test was performed in triplicate samples of uncoated (control) and coated stones, by using the climatic chamber Suntest XXL+ from Atlas in order to test the weather resistance of coatings applied on different stone types by a simulation of drastic and worst climatic conditions (strong irradiance, storm rain) than the moderate oceanic climate of the Reims region, through sunlight, rainfall, temperature and humidity. The device is equipped with three 1700 W air-cooled Xenon Lamps to simulate daylight with the control of irradiance 300–400 nm. Chamber temperature (CHT), black standard temperature (BST) and the relative humidity (RH) were set up and controlled. Rainfall was simulated by a spray system with two nozzles (Schlick nozzle 11–90° = 420 mL/nozzle/min). 21 cycles were performed, one cycle lasted 12 h with a succession of periods of high temperature (50 °C), high relative humidity (80 %), irradiance at 55 W/m² for 6 h per cycle corresponding to 1 month of real exposure in Southern France (conversion given by Atlas company), followed by 1 h of heavy rainfall which corresponded to 168 mm (Fig. S2). The samples were exposed for 252 h (10.5 days).

2.4.2. Accelerated biocolonisation test

Stone triplicates aged by the previous weathering test were submitted to a biocolonisation test in a climatic test chamber VC³ 4034 (Vötsch), to verify the biocidal efficiency of POM-IL coatings after harsh climatic conditions. Slabs were inoculated by spraying out

1 mL suspension of *Pseudostichococcus monallantoides* green alga (OK432519) (Eyssautier-Chuine et al., 2018; Franco-Castillo et al., 2022; Sasso et al., 2016) cultivated from an isolated natural strain in a liquid medium composed of sterile distilled water and Hoagland medium (Table S1). The algal suspension was diluted to obtain a concentration of around 120 cells/0.1 μL and checked by the chlorophyll *a* absorbance control at 665 nm using spectrophotometry (Thermo Fisher Scientific Genesys 10-S). Each slab was placed in a Plexiglass cup and 20 mL of Hoagland medium was provided from the bottom to get wetted slabs. A transparent lid on every cup limited the evaporation and the medium was added one a week for porous stones and twice a week for non-porous stones over the test to get around 5 mL of liquid in the bottom of cups the goal was to keep a wetness on porous and non-porous stone surfaces. The incubation lasted five weeks with 20 °C, 80 % relative humidity and 12 h daylight per 24 h ensured by two fluorescent lights (Sylvania Gro-Lux-15 W lamp, PAR = 25 mmol (photons) $\text{m}^{-2}\cdot\text{s}^{-1}$). The biocolonisation of slabs was measured by colorimetry and *chlF*.

2.4.3. Outdoor biocolonisation test

The natural outdoor biocolonisation of POM-IL-coated and uncoated stones was evaluated over a two-year period (Nov. 2019–Nov. 2021) in a private garden with trees in Reims city (Eastern France) (49°14'18.4"N 4°03'43.3"E) corresponding to temperate climate (Table S2). Triplicates of coated and uncoated stones (controls) and were left tilted at 30° in a rack facing South. The monitoring of the biocolonisation on the samples was carried out every two months by non-destructive techniques (colorimetry and *chlF*). Sample surfaces were beforehand wet by spraying distilled water to avoid the artefact that the variation of water content in stones through the seasons could generate on the colour measurements like the darkening of the stone surface instead of the biocolonisation.

2.5. Statistical analysis

The open-source software R.4.2.1 (R Core Team, 2014) has been used to compute statistics and to produce all graphics, with the following packages: ggplot2 (Wickham, 2009), R. utils (Bengtsson, 2016), doBy (Højsgaard and Halekoh, 2016), readxl (Wickham, 2016). Gaussian distributions of colorimetric and *chlF* fluorescence parameters were achieved independently then ANOVA tests were generated to define the statistical significance level *p*-values between data from control stones and data from coated stones (no significant difference (no letter): $p > 0.05$; significant difference with $p < 10^{-4}$ (a), $p < 0.001$ (b), $p < 0.01$ (c), $p < 0.05$ (d)). The water vapour permeability data were analysed with the non-parametric Mann and Whitney *U* test at the 0.05 probability level between control (uncoated stones) and coated stones.

3. Results

3.1. Stone surface characterization after treatment

3.1.1. Colour variation

Overall, we observed a darkening (decrease of ΔL^*) and a yellowing (increase of Δb^*) of the stones. Of the four POM-IL-coated stones, the calculated ΔE^*_{ab} was lowest for SA at 3.3 and 2.9 for POM-IL1 and 2, respectively (Fig. 1 and Table S3). ΔE^*_{ab} for DO were at 4.8 and 4.4 that is high but values were close to data obtained for this stone in another study (Eyssautier-Chuine et al., 2018). RO and BB, which have a natural dark colour, both had ΔE^*_{ab} between 14.6 and 18.1, which can be explained by the strong decrease of ΔL^* and further darkening of the stones.

3.1.2. Variation of the porous network

The microstructural characteristics of uncoated and coated stones were assessed through the mercury (Hg) intrusion measurements to evaluate how coating application can modify the porous network, saturating the

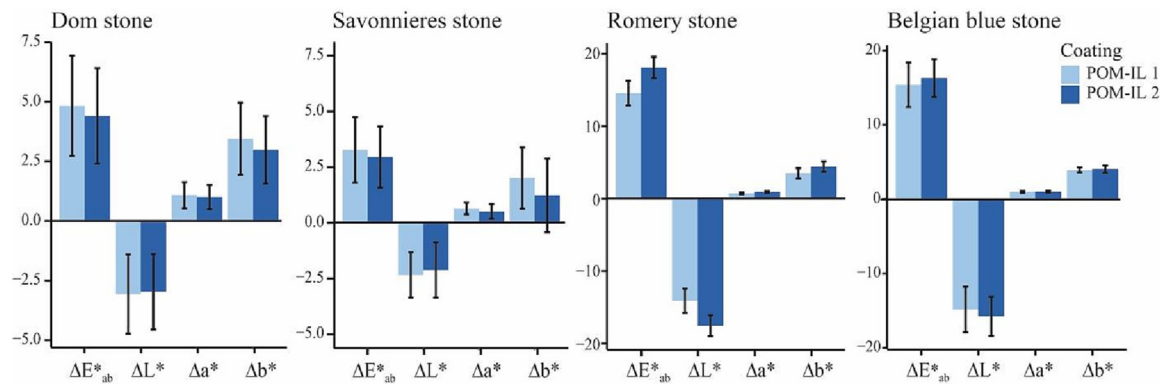


Fig. 1. Colour variations (ΔE^*_{ab} , ΔL^* , Δa^* , Δb^*) at the stone surface calculated with the colour measured before POM-IL1 and POM-IL2 coating application and after the application of coatings.

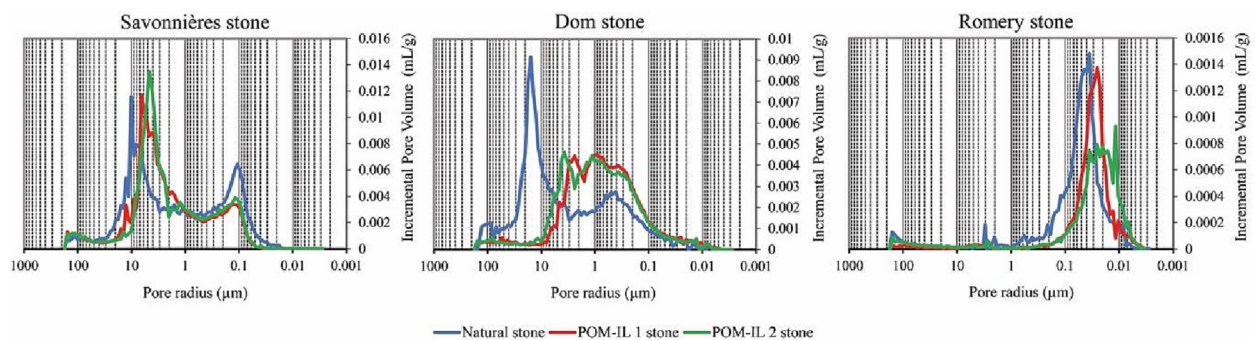


Fig. 2. Incremental mercury intrusion in relation to the pore size for the porous stones. Comparison of the pore access radii distribution of the natural stone and the POM-IL1 and POM-IL2 coated stones.

stones with a large amount of product. Only the BB porous network was not measured because its porosity is below the limit of detection of this technique (Fig. 2, Table S4). The natural porosity of DO (29.1 %) decreased to 26.8 % for the POM-IL1 stone and 28.4 % for POM-IL2 stone. The macropore ($>10 \mu\text{m}$) access radius decreased drastically for both coated stones and an increase in the smaller pore sizes (between 10 and $0.1 \mu\text{m}$) was observed. For SA (34.9 % porosity), the porosity of POM-IL1 stone was close to the uncoated stone and decreased a little for the POM-IL2-

coated stone (32.4 %). Overall, there was a low global impact of coatings on the porosity of these porous stones. The pore network change was noticed by a shift of the macropore size from $10.3 \mu\text{m}$ to 4.7 and $5 \mu\text{m}$ for POM-IL stones that fostered to a decrease of the quantity of pores $>10 \mu\text{m}$ access radius and an increase of pores between 10 and $1 \mu\text{m}$. We also observed a decrease in the number of small pores ($1-0.1 \mu\text{m}$ and $<1 \mu\text{m}$ access radius). For RO, the initial weak porosity of 4.8 % decreased slightly to 4.1 % and 3.2 % for stones coated with POM-IL1 and POM-IL2,

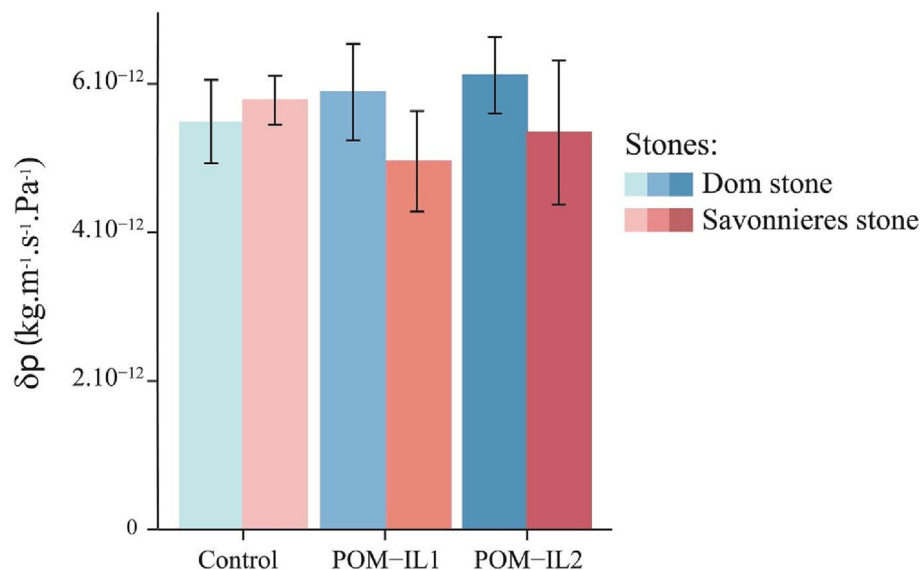


Fig. 3. Water vapour permeability (δp) with respect to partial vapour pressure ($\text{kg.m}^{-1}.\text{s}^{-1}.\text{Pa}^{-1}$).

respectively. The major microporosity with pores size at $0.06\ \mu\text{m}$ lowered to $0.03\ \mu\text{m}$ for POM-IL2 stone, where the number of pores slightly decreased in comparison with the uncoated stone.

3.1.3. Permeability to water vapour

The water vapour permeability of four natural DO and SA samples (control) were compared to four POM-IL1 and four POM-IL2-coated samples. Statistical analysis (non-parametric Mann and Whitney *U* test) confirmed that there was no significant variation between control and POM-IL-coated stones (Fig. 3).

3.2. Testing POM-IL durability on stones through a simulation of drastic weather

3.2.1. Colour variation

Triplicates of POM-IL-coated and uncoated (control) stones were subjected to 21 climatic cycles, then colour variations of the upper stone surface were calculated from the colour before and after the test. For Dom stone, ΔE^*_{ab} as the global colour change was 6.8 for control, in particular the stone tended to be yellower ($\Delta b^* = 4.7$) and less red ($\Delta a^* = -4.2$) (Fig. 4 and Table S5). ΔE^*_{ab} of coated stones were similar to ΔE^*_{ab} of control with 7.2 and 6.6 respectively for POM-IL1 and POM-IL2, coated stones were less red ($\Delta a^* = -5.5$ and -5.4) like control, while the yellowing was lower than control ($\Delta b^* = 1.7$ and 1.9). ΔL^* increased for both POM-ILs, so they were slightly clearer than control. For SA, the colour trends were similar to DO, ΔE^*_{ab} of control and coated stones had the same increase after the weathering (7.1 and 6.9). There was a similar decrease of Δa^* , but Δb^* was lower for POM-IL stones (1.6 and 2.4) instead of 4.3 for control,

thus the yellowing of stones was less evident than that of the control. Moreover, ΔL^* increased for coated stones (2.7 and 2.4) thus POM-IL stones were clearer after the weathering whereas control ΔL^* tended to decrease (-1.7) thus control was slightly darker than before the weathering test.

Controls of RO and BB had an increase of ΔE^*_{ab} of 7.5 for RO and 4.5 for BB. For RO, this result is associated to a lighter ($\Delta L^* = 43.9$) and a yellower ($\Delta b^* = 4.3$) appearance, whereas for BB controls, the global colour variation was only linked to a lightening of the stone with ΔL^* of 3.8. ΔE^*_{ab} of both coated stones was between 15.1 and 18.3 thus the colour changed strongly after the test mostly due to a high ΔL^* (14.4 and 16.8 for RO, 16.0 and 17.8 for BB respectively for POM-IL1 and POM-IL2) so a lightening of the stones, more important than observed on controls.

3.2.2. EDX analysis of POM-IL-coated stones

EDX detected Tungsten from the polytungstate anion, $[\text{a-SiW}_{11}\text{O}_{39}]^{8-}$, used to form both POM-ILs. The % W on the four types of stone ranged from 1.20 % on SA to 6.53 % on BB (Fig. S3) providing an indication of the durability of the coatings following the simulated weathering tests.

3.3. Testing of the anti-algal activity of POM-ILs with aged stones

3.3.1. Δa^* variation

The efficiency of POM-ILs was firstly evaluated by the monitoring of the colour change of stones and specifically by the greening through Δa^* (Fig. 5 - Fig. S4), the average and the deviation standard were reported in Table S6. During the 5-week incubation, DO controls displayed no colour change at

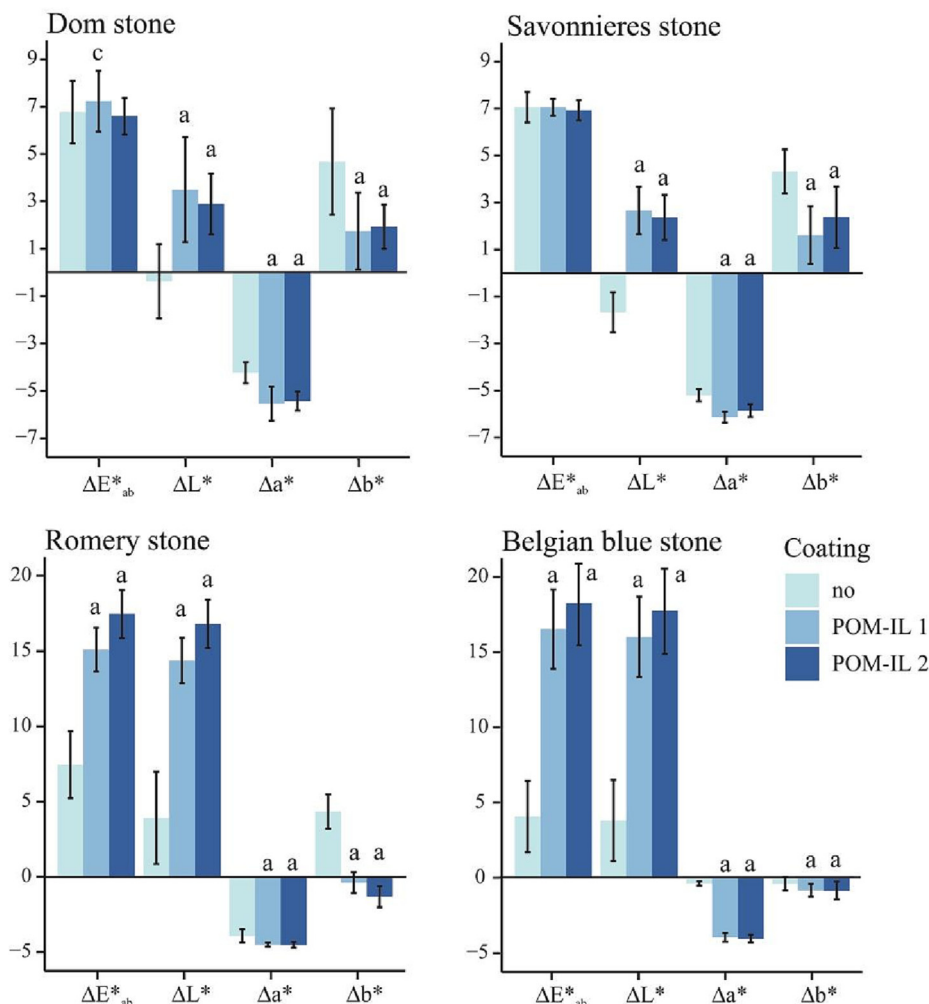


Fig. 4. Colour variations (ΔE^*_{ab} , ΔL^* , Δa^* , Δb^*) of the four stones on control and POM-IL1 and POM-IL2 coated stones after ageing by the simulated climatic test.

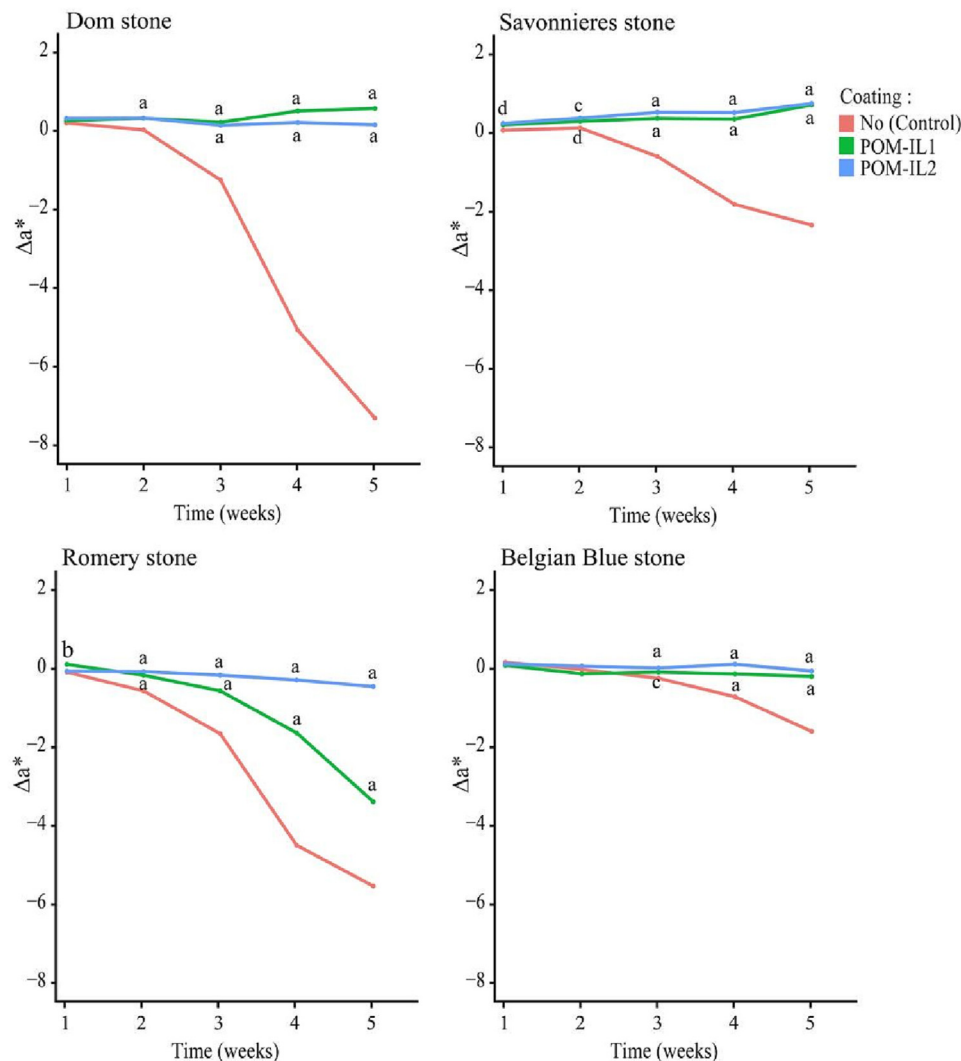


Fig. 5. Δa^* colour variations of Dom, Savonnières, Romery and the Belgian Blue stone during the five-week accelerated biocolonisation test showing the control, anti-algal activity of POM-IL1 and POM-IL2 samples that had previously been aged in the simulated climatic test.

week 1 and 2. Δa^* decreased and was negative with -1.3 from week 3 until the end of the experiment where Δa^* of -7.3 , which showed a greening of the stones. In comparison, both POM-IL1 and 2 stayed close to 0 that disclosed no colour change thus no greening. SA showed a similar trend that DO, a decrease of Δa^* started at week 3 until week 5 nonetheless, the greening was less significant than on DO since Δa^* was at -2.4 at the end of the test for SA and -7.3 for DO. Δa^* of POM-IL slabs had a weak increase, between 0.2 and 0.7 that displayed no greening of the stones. On RO and BB which are not porous, the growth of algae was carried on by a high humidity in the Petri dishes thanks to a constant medium at the bottom of slabs which rose to the surface by the weak capillarity of the stone or by evaporation of the water. On RO controls, Δa^* decreased progressively through time from -0.1 at week 1 to -5.5 at week 5 which displayed a greening. For POM-IL1, Δa^* decreased from week 2 with -0.1 to -3.4 at week 5. There was a progressive greening of the slabs even if it was less pronounced than on controls. POM-IL2 Δa^* displayed very weak values over the test to the end which showed a weak greening. With BB stones, Δa^* of controls decreased slightly to -1.6 at week 5, whereas on POM-IL1 and 2 stones, the values were close to 0 until the end of the experiment.

3.3.2. Chlorophyll a fluorescence

Biocide treatments can generate such a stress that chlF can detect and show by a decrease of photosystem II efficiency (F_v/F_m) in the

photosynthetic chain. At week 5 of the experiment, F_v/F_m of controls were at 0.65 and 0.64 for DO, RO and BB and at 0.54 for SA (Fig. 6). On DO and SA coated stones, F_v/F_m was much weaker than controls and was 0.30 and 0.33 for DO, and 0.19 and 0.17 for SA. Therefore, results revealed a weaker photosynthetic activity on stones treated by POM-IL1 and 2. On RO, F_v/F_m remained as high as controls on POM-IL1 with 0.66 and a little lower on POM-IL2 with 0.53, thus the photosynthetic activity was similar on POM-IL1 than controls and it decreased on POM-IL2 but much less than on DO and SA. Finally, on BB, F_v/F_m was 0.48 for POM-IL1 and 0.37 for POM-IL2, the photosynthetic activity with the coatings decreased compared to the controls but remained higher than on DO and SA.

3.4. Outdoor biocolonisation test

The biocidal activity of POM-IL coating on the four stone variants was assessed by exposing the stone slabs to all four seasons of the year over a two-year period in an outdoor environment in Reims, north-east France (Fig. S5). This two-year-long experiment was used to study the natural seeding and biocolonisation of the stone slabs and evaluate the activity of the POM-IL biocides. This process was carried out in parallel to the climate chamber tests, which subjected the coatings to a succession of severe climatic conditions to evaluate the response of the coatings to climate change, where global climatic conditions are going to be much harsher, then to a biocolonisation with algal species.

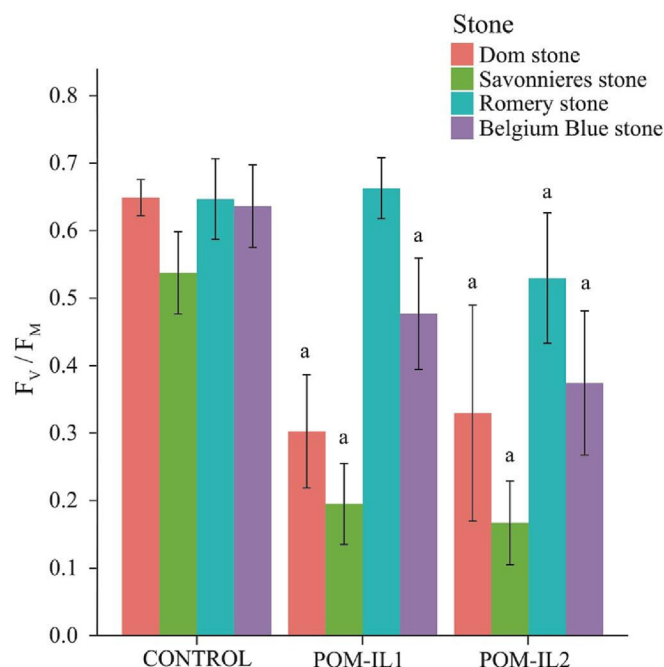


Fig. 6. Chl.a fluorescence (F_v/F_m) measured on Dom, Savonnieres, Romery and the Belgian Blue stone on aged control and aged POM-IL1 and POM-IL2 stones after the five-week accelerated biocolonisation test.

3.4.1. Colour variation

After two years of natural ageing in an outdoor environment, the colour of both the coated and uncoated porous SA and DO stones changed significantly (Fig. 7 and Table S7). The ΔL^* and Δa^* values were similar for both the control and POM-IL-coated stones. Over the two-year period of study, the colour of stones tended to darken and, in addition, an increase in Δb^* in the POM-IL coated SA and DO indicated a gradual greening and yellowing over time, when compared to control stones. The RO stone was also characterised by a high Δb^* (from 5.8 to 6.1) for both control and POM-IL-coated samples, indicating a gradual yellowing. Finally, there was no appreciable variation in colour for BB following the two-year exposure to outdoor climates.

3.4.2. Chlorophyll a fluorescence

Results displayed similar F_v/F_m values between controls and coated stones for the four types of stone, indicating that a similar photosynthetic activity was detected thus POM-ILs were not efficient enough to resist biocolonisation of phototrophic microorganisms after two years of exposure outdoors (Fig. 8). However, it seems that the POM-IL coatings were still active after one year. Taking the SA stones as an example, monitoring every two months showed a net increase of the PSII efficiency of 0.38 on the control samples (in December 2020; month 14), which was not observed on POM-IL stones, indicating that the coatings were still active after one year (Fig. S6).

3.4.3. SEM observations of coated stones

SEM was used to provide a qualitative analysis of the biological colonisation of the stones following the two-year exposure period (Fig. 9 and Fig. S7-S9). All uncoated stones showed significant biological colonisation (Fig. S9). For the POM-IL-coated stones, porous DO and SA stones showed development of fungal mycelium. Low porosity RO and non-porous BB stone coated with POM-ILs showed almost no evidence of biocolonisation, only a few signs of mycelium growth and isolated cells (Fig. 9 and Fig. S7-S8).

4. Discussion

The first step of this study was to assess the effect of the application of POM-ILs on the stone colour and properties. The global colour variation (ΔE^*_{ab}) threshold was established as $\Delta E^*_{ab} \leq 3$, which has been defined by our previous work and other authors who have applied biocidal coatings on stones with similar appearance to Savonnieres (Burgos-Cara et al., 2017; Franco-Castillo et al., 2022; Moreau et al., 2008). In our study, the colour change induced by the coatings was under the threshold for SA and close to 5 for DO, so higher than the threshold but it was in accordance with the other studies. On RO and BB, the biocides were too high to be considered as protective coatings for stone-based heritage. This result revealed that the biocidal POM-IL products do not absorb and penetrate inside RO and BB, which are weakly and not porous, respectively. On the other hand, water vapour permeability tests revealed that POM-IL coatings did not significantly alter the water vapour permeability through DO and SA, making these coatings highly promising for the effective biocidal protection of stone heritage constructed from porous mineral stone. The analysis of the pore network of DO, SA and RO, for which the amount of POM-ILs was excessively increased, displayed how both coatings produced a moderate

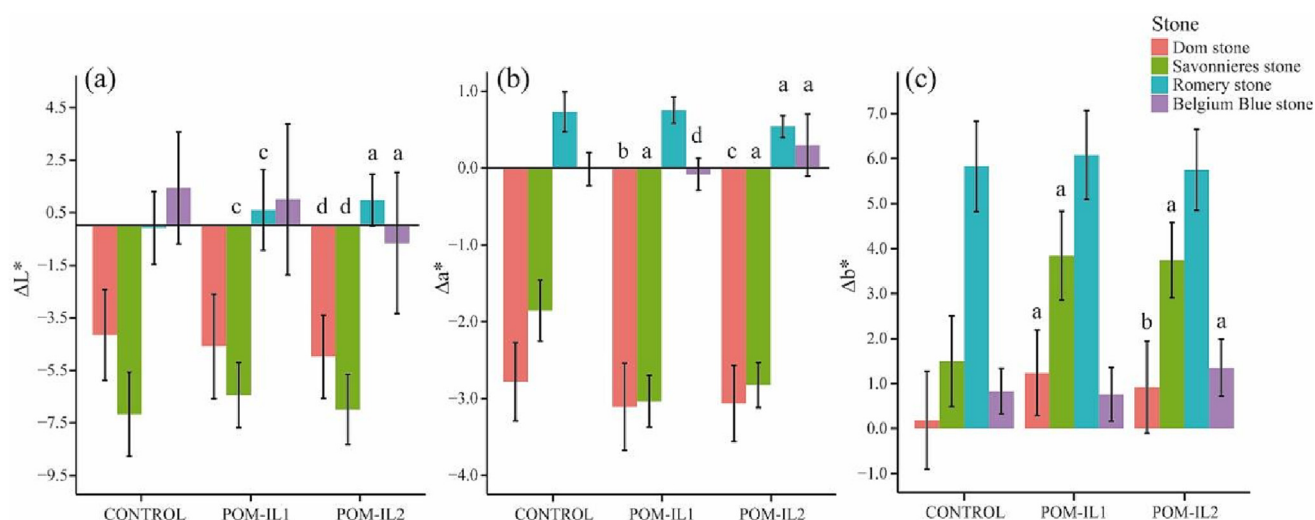


Fig. 7. Variation of colour parameters: (a) ΔL^* ; (b) Δa^* and (c) Δb^* , for the four types of stone between the beginning and at the end of the experiment (two years). Mean and standard deviation values were calculated from triplicates of controls (uncoated stones) and POM-IL1 and POM-IL2 coated stones.

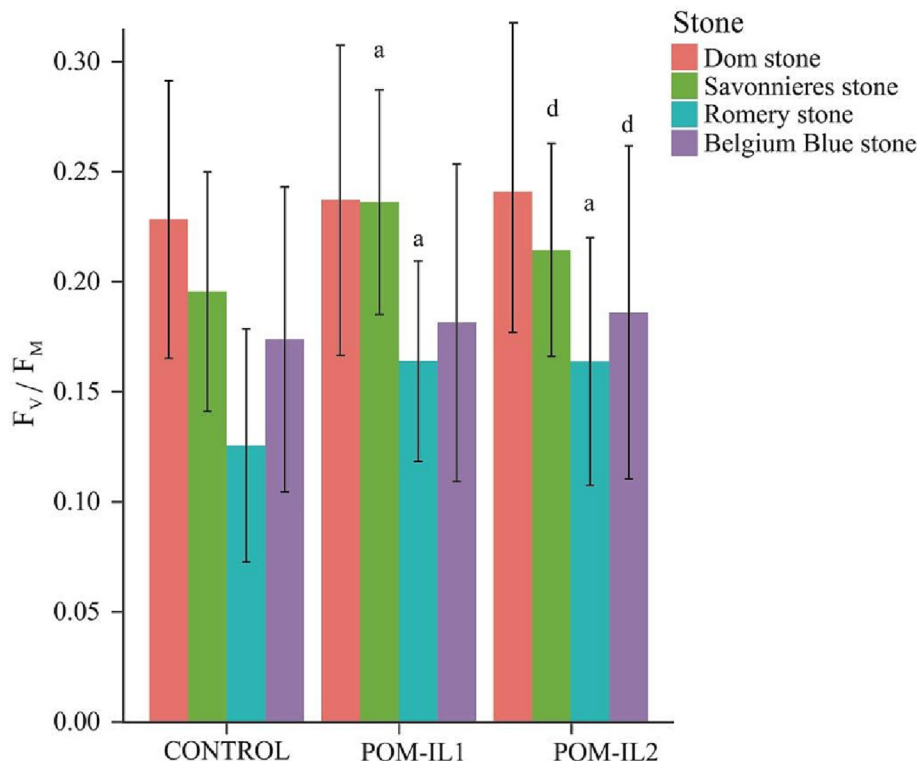


Fig. 8. F_v/F_m of the four types of stone after two years of experiment. Mean and standard deviation values were calculated from triplicates of controls (uncoated stones) and POM-IL1 and POM-IL2-coated stones.

reduction in the macropore size of DO and decreased the SA micropores. This suggests that the coatings tended to partially seal macropores and thus to decrease the pore sizes and their quantity.

The climatic tests aimed to evaluate POM-IL coatings under harsh climatic conditions which could simulate future events predicted by current climate models (Jacob et al., 2014; Jones et al., 2009). In particular, the test was designed with an irradiance close to that experienced in the south of France, with high temperature (40 °C). The BST (black panel) reached as high as 60 °C meaning that the darker coloured stone surfaces BB, DO and RO reached this temperature. High temperature exposure was directly followed by heavy rainfall with a water flow similar to a thunderstorm, which is similar to the summertime weather in the south of France.

The colour of all natural uncoated stones (controls) changed following the climate chamber test; thus the weather had a net impact on all types of stone whatever the initial colour (Eyssautier-Chuine et al., 2018). Comparison of control and coated stones displayed two trends of colour variation: (i) in the case of DO and SA where the global colour

change was the same for control and coated stones. This result suggested that similar intrinsic properties of stones (high porosity, capillarity, roughness) benefitted the penetration of the biocide into the substrates and played an important role on the durability of the coatings. And (ii) in the case of RO and BB, since the application of POM-ILs led to their darkening and since the weathering produced a gradual lightening, the final colour of coated stones actually became close to the natural colour of uncoated stones (Table S8). This result was only observed for the non-porous stones for which there was a weak penetration of the products inside the substrate, raising the question of the coating's adhesion to the stone thus of durability and efficiency in the face of severe weather. EDX analysis detected the residual presence of tungsten from the POM anion on coated stones after the weathering test in climatic chamber, indicating that POM-ILs were still embedded within the stones after the weather ageing. The accelerated biocolonisation test using green algae on aged, coated stones provided an answer to whether the quantity of such coatings could be enough to deter algal colonisation. Colour data displayed neither greening nor yellowing of coated slabs

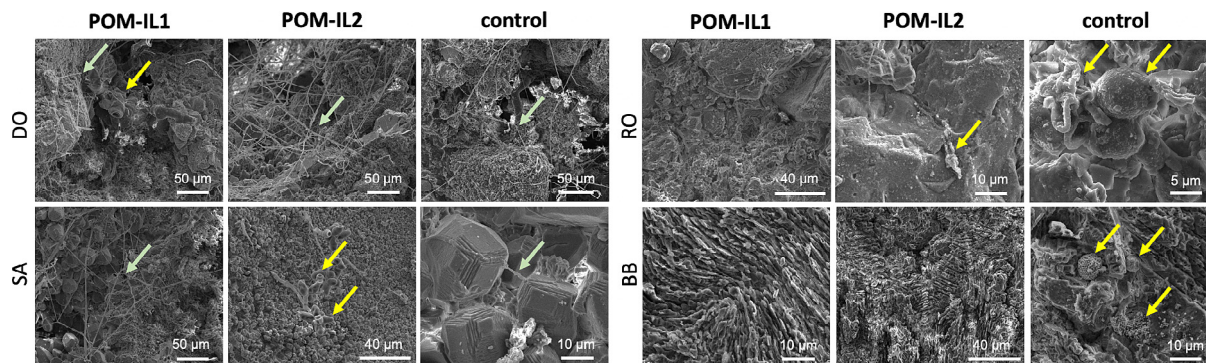


Fig. 9. SEM images showing biological development on stone slabs after two years exposure outdoors in Reims (north east France). yellow arrows indicate spores or cells; green arrows indicate fungal mycelium.

for DO, SA and BB, indicating an absence of algal development on the stone surface and an efficient anti-algal activity of both POM-ILs. However, a minor greening was detected on POM-IL-coated RO (Fig. S4). ChlaF analysis through F_V/F_M , provided a more in-depth insight into the effect of the POM-ILs on the physiological status of algae since the photosystem II (PSII) of the photosynthetic chain is sensitive to environmental stress. ChlaF was detected on every coated stone thus this photosynthetic activity suggested that algae were still alive but the maximum quantum yield of PSII of POM-IL-coated DO and SA stones decreased significantly compared with controls which infers those coatings had detrimental impact on the PSII of the algae. Nonetheless, this effect had also been detected on BB to a lesser extent and on RO with POM-IL2. Accordingly, after the drastic climatic test, both POM-IL1 and 2 retained their anti-algal activity on all four stones. Both POM-IL1 and POM-IL2 had an equivalent efficiency on DO and SA stones probably due to their high porosity which promoted an improved penetration of POM-ILs as it was already reported with tufa and marble coated with ILs (De Leo et al., 2021). However, On RO and BB, POM-IL2 was more efficient than POM-IL1.

The two-year outdoor exposure test was carried out in parallel to the simulated climate chamber weathering and accelerated biocolonisation tests. Colour results of both DO and SA for control and POM-ILs displayed a darkening which were induced by a fungal growth (SEM observations). A gradual greening and a yellowing was also observed by colorimetry measurements and was associated to phototrophs such as algae and cyanobacteria, which were detected by chaF and constitute the main photosynthetic microorganisms colonizing stones. Nonetheless, F_V/F_M values were weak, indicating a low phototrophic growth on stones probably due to the competition with other microorganisms. However, after the climatic lab test, a natural greening and yellowing colour change to DO, SA and RO was also observed meaning that such alterations could be the natural result of outdoor exposure. SEM analysis suggested that the POM-ILs were not efficient enough to fully inhibit the biocolonisation of the four stones over this period (Fig. 9 and Fig. S7-S9). In particular, the porous stones DO and SA showed signs of typical outdoor colonisers such as moulds and phototrophic microorganisms, whereas virtually no microorganism growth was found on weakly porous RO or non-porous BB. A previous study testing the efficiency of POM-IL1 and 2 against bacteria (*E. coli*) on BB, RO and DO had the best result with POM-IL1 on BB (Misra et al., 2018). In addition, a better anti-fungal activity was already proved on brick with POM-ILs with a higher number of C atoms of alkyl substituents, such as POM-IL2 (Rajkowska et al., 2020). Altogether, these results suggest that a higher amount of POM-IL should be applied to non-porous stones to prevent long-term biocolonisation in outdoor environments. Importantly, colour studies and water vapour permeability data support the idea that higher concentrations of POM-IL could be applied instead of increasing the amount, with no deleterious cosmetic or physical effect to the stone to avoid impacting the porous network. Furthermore - and in contrast to the results from porous DO and SA stones - even lower concentrations and total amount of POM-IL could be applied to less porous mineral stones such as RO and BB.

5. Conclusions

Our aim has been to develop custom-made antifouling solutions based on POM-ILs and perform an in-depth analysis of their capacity to prevent biocolonisation of calcareous stones in simulated and outdoor environments. POM-IL coatings did not affect water vapour permeability and only moderately reduced the total porosity of the calcareous stones. The colour variation of POM-IL-coated stones following a period of simulated weathering in climate chambers - simulating harsh (hot and wet) climatic weather conditions - did not vary significantly with respect to the natural uncoated stones. Crucially, accelerated biocolonisation studies on weathered POM-IL-coated stones were still capable of preventing biocolonisation by an algal biofilm. However, while colour measurements and chlorophyll fluorescence data obtained

over a two-year period of ageing outdoors in northern France were promising, scanning electron microscopy imaging of the stones highlighted that coated and uncoated stones showed signs of colonisation by fungal mycelium and phototrophic cells. Consequently, while our results demonstrate that POM-ILs appear to be suited to deployment as preventative biocidal coatings for calcareous stones, the microstructural/porosity features of different types of calcareous stones play a significant role in the overall performance of the coatings. In this respect, the correct concentrations must be carefully chosen to achieve a balance between colour variation and biocidal effect over longer periods of time, particularly in outdoor environments.

CRedit authorship contribution statement

The idea for the work was conceived by SEC and SGM. Materials preparation was performed by IFC and AM under the supervision of SGM and CS. Coating of stones with POM-ILs was made by SGM and IFC. Analysis of stones, microbiology experiments, climate chamber experiments, outdoor studies, and all corresponding sample monitoring was carried out by SEC, with assistance from JH and NVG. SEM/EDX was performed by SGM and SEC. The main hypothesis development and data analysis were undertaken by SEC and SGM. The first draft of the manuscript was written by SEC and SGM. All authors reviewed and edited the final version of the manuscript and approved its submission.

Data availability

Data will be made available on request.

Declaration of competing interest

The authors declare the following financial interests/personal relationships which may be considered as potential competing interests:

Scott G. Mitchell reports financial support was provided by Ministerio de Ciencia e Innovación Agencia Estatal de Investigación. Isabel Franco Castillo reports financial support was provided by Programa Operativo Aragón de Fondo Social Europeo 2014–2020. Scott G. Mitchell reports financial support was provided by Fondo Social del Gobierno de Aragón. Scott G. Mitchell reports administrative support was provided by Servicio General de Apoyo a la Investigación-SAI. Scott G. Mitchell reports administrative support was provided by Laboratorio de Microscopías Avanzadas at University of Zaragoza. Scott G. Mitchell reports administrative support was provided by Interdisciplinary Thematic Platform from CSIC Open Heritage Research and Society (PTI-PAIS).

Acknowledgements

This work was funded through the grant PID2019-109333RB-I00 funded by MCIN/AEI/10.13039/501100011033 (Ministerio de Ciencia e Innovación/Agencia Estatal de Investigación, Spain) and was supported by MCIN with funding from European Union NextGenerationEU (PRTR-C17.I1) promoted by the Government of Aragón. The authors also acknowledge the Fondo Social del Gobierno de Aragón (grupo DGA E15.20R) and the Programa Operativo Aragón de Fondo Social Europeo 2014-2020 (I.F.C.). The authors acknowledge the Servicio General de Apoyo a la Investigación-SAI (Universidad de Zaragoza), for the use of instrumentation as well as the technical advice provided by the National Facility ELECMI ICTS, node “Laboratorio de Microscopías Avanzadas” at University of Zaragoza. The authors wish to acknowledge professional support of the Interdisciplinary Thematic Platform from CSIC Open Heritage: Research and Society (PTI-PAIS).

Appendix A. Supplementary data

Supplementary data to this article can be found online at <https://doi.org/10.1016/j.scitotenv.2023.163739>.

References

- Alisi, C., 2011. Biodegradation and bioremediation of stone manufacts. *Lecture Di Georisorse e Ambiente*. Presented at the Minerals and Biosphere, Campiglia Marittima, pp. 94–109.
- Bartoli, F., Muncichia, A.C., Futagami, Y., Kashiwadani, H., Moon, K.H., Caneva, G., 2014. Biological colonization patterns on the ruins of Angkor temples (Cambodia) in the biodegradation vs bioprotection debate. *Int. Biodeterior. Biodegrad.* 96, 157–165. <https://doi.org/10.1016/j.ibiod.2014.09.015>.
- Becerra, J., Ortiz, P., Zaderenko, A.P., Karapanagiotis, I., 2020. Assessment of nanoparticles/nanocomposites to inhibit micro-algal fouling on limestone façades. *Build. Res. Inform.* 48, 180–190. <https://doi.org/10.1080/09613218.2019.1609233>.
- Bengtsson, H., 2016. Rutils: Various Programming Utilities. R Package Version 2.5.0. <https://CRAN.R-project.org/package=Rutils>.
- Bertuzzi, S., Gustavs, L., Pandolfini, G., Tretiach, M., 2017. Heat shock treatments for the control of lithobionts: a case study with epilithic green microalgae. *Int. Biodeterior. Biodegradation* 123, 236–243. <https://doi.org/10.1016/j.ibiod.2017.06.023>.
- Bijelic, A., Aureliano, M., Rompel, A., 2018. The antibacterial activity of polyoxometalates: structures, antibiotic effects and future perspectives. *Chem. Commun.* 54, 1153–1169. <https://doi.org/10.1039/C7CC07549A>.
- Brunelli, A., Calgaro, L., Semenzin, E., Cazzagon, V., Giubilato, E., Marcomini, A., Badetti, E., 2021. Leaching of nanoparticles from nano-enabled products for the protection of cultural heritage surfaces: a review. *Environ. Sci. Eur.* 33–48. <https://doi.org/10.1186/s12302-021-00493-z>.
- Burgos-Cara, A., Ruiz-Agudo, E., Rodriguez-Navarro, C., 2017. Effectiveness of oxalic acid treatments for the protection of marble surfaces. *Mater. Des.* 115, 82–92. <https://doi.org/10.1016/j.matdes.2016.11.037>.
- Carrapiço, A., Martins, M.R., Caldeira, A.T., Mirão, J., Dias, L., 2023. Biosynthesis of metal and metal oxide nanoparticles using microbial cultures: mechanisms, antimicrobial activity and applications to cultural heritage. *Microorganisms* 11, 378. <https://doi.org/10.3390/microorganisms11020378>.
- Colangiuli, D., Lettieri, M., Masieri, M., Calia, A., 2019. Field study in an urban environment of simultaneous self-cleaning and hydrophobic nanosized TiO₂-based coatings on stone for the protection of building surface. *Sci. Total Environ.* 650, 2919–2930. <https://doi.org/10.1016/j.scitotenv.2018.10.044>.
- Coutinho, M.L., Miller, A.Z., Martin-Sanchez, P.M., Mirão, J., Gomez-Bolea, A., Machado-Moreira, B., Cerqueira-Alves, L., Jurado, V., Saiz-Jimenez, C., Lima, A., 2016. A multiproxy approach to evaluate biocidal treatments on biodeteriorated majolica glazed tiles. *Environ. Microbiol.* 18, 4794–4816. <https://doi.org/10.1111/1462-2920.13380>.
- Cronin, L., Müller, A., 2012. From serendipity to design of polyoxometalates at the nanoscale, aesthetic beauty and applications. *Chem. Soc. Rev.* 41, 7333–7334. <https://doi.org/10.1039/C2CS90087D>.
- Daima, H.K., Selvakannan, P.R., Kandjani, A.E., Shukla, R., Bhargava, S.K., Bansal, V., 2014. Synergistic influence of polyoxometalate surface corona towards enhancing the antibacterial performance of tyrosine-capped ag nanoparticles. *Nanoscale* 6, 758–765. <https://doi.org/10.1039/C3NR03806H>.
- De Leo, F., Marchetta, A., Capillo, G., Germanà, A., Primerano, P., Schiavo, S.L., Urzi, C., 2021. Surface active ionic liquids based coatings as subaerial anti-biofilms for stone built cultural heritage. *Coatings* 11, 26. <https://doi.org/10.3390/coatings11010026>.
- Di Martino, P., 2016. What about biofilms on the surface of stone monuments? *Open Conf. Proc. J.* 7. <https://doi.org/10.2174/2210289201607020014>.
- European Committee for Standardization, 2010. NF EN 15803 - Mars 2010 - Conservation of Cultural Properties. Test Methods. Determination of Water Vapour Permeability. La Plaine Saint-Denis.
- European committee for Standardization, 2011. CSN EN ISO 11664-4 - Colorimetry - Part 4: CIE 1976 L*a*b* Colour space (ISO 11664- 4:2008), Category: 0117 Optics. <https://www.En-Standard.Eu>.
- Eyssautier-Chuine, S., Calandra, I., Vaillant-Gaveau, N., Fronteau, G., Thomachot-Schneider, C., Hubert, J., Pleck, J., Gommeaux, M., 2018. A new preventive coating for building stones mixing a water repellent and an eco-friendly biocide. *Progress in Organic Coatings* 120, 132–142. <https://doi.org/10.1016/j.porgcoat.2018.03.022>.
- Eyssautier-Chuine, S., Vaillant-Gaveau, N., Charpentier, E., Refeuille, F., 2021. Comparison of biofilm development on three building and restoration stones used in french monuments. *Int. Biodeterior. Biodegradation* 165, 105322. <https://doi.org/10.1016/j.ibiod.2021.105322>.
- Favero-Longo, S.E., Benesperi, R., Bertuzzi, S., Bianchi, E., Buffa, G., Giordani, P., Loppi, S., Malaspina, P., Matteucci, E., Paoli, L., Ravera, S., Roccardi, A., Segimiro, A., Vannini, A., 2017. Species- and site-specific efficacy of commercial biocides and application solvents against lichens. *Int. Biodeterior. Biodegradation* 123, 127–137. <https://doi.org/10.1016/j.ibiod.2017.06.009>.
- Franco-Castillo, I., Hierro, L., Jesús, M., Seral-Ascaso, A., Mitchell, S.G., 2021. Perspectives for antimicrobial nanomaterials in cultural heritage conservation. *Chem* 7, 629–669. <https://doi.org/10.1016/j.jchempr.2021.01.006>.
- Franco-Castillo, I., Misra, A., Laratte, S., Gommeaux, M., Perarnau, R., Vaillant-Gaveau, N., Pierlot, C., Streb, C., Mitchell, S.G., Eyssautier-Chuine, S., 2022. New protective coatings against lampenflora growing in the pommary champagne cellar. *Int. Biodeterior. Biodegradation* 173, 105459. <https://doi.org/10.1016/j.ibiod.2022.105459>.
- Gómez-Ortiz, N.M., González-Gómez, W.S., De la Rosa-García, S.C., Oskam, G., Quintana, P., Soria-Castro, M., Gómez-Cornelio, S., Ortega-Morales, B.O., 2014. Antifungal activity of Ca [Zn(OH)3]2H₂O coatings for the preservation of limestone monuments: an in vitro study. *Int. Biodeterior. Biodegradation* 91, 1–8. <https://doi.org/10.1016/j.ibiod.2014.02.005>.
- Hallett, J.P., Welton, T., 2011. Room-temperature ionic liquids: solvents for synthesis and catalysis. 2. *Chem. Rev.* 111, 3508–3576. <https://doi.org/10.1021/cr1003248>.
- Herrmann, S., Kostrowska, M., Wierschem, A., Streb, C., 2014a. Polyoxometalate ionic liquids as self-repairing acid-resistant corrosion protection. *Angew. Chem. Int. Ed.* 53, 13596–13599. <https://doi.org/10.1002/anie.201408171>.
- Herrmann, S., Seliverstov, A., Streb, C., 2014b. Polyoxometalate-ionic liquids (POM-ILs)—the ultimate soft polyoxometalates? A critical perspective. *J. Mol. Eng. Mater.* 2, 1440001. <https://doi.org/10.1142/S2251237314400012>.
- Herrmann, S., De Matteis, L., de la Fuente, J.M., Mitchell, S.G., Streb, C., 2017. Removal of multiple contaminants from water by polyoxometalate supported ionic liquid phases (POM-SILPs). *Angew. Chem. Int. Ed.* 56, 1667–1670. <https://doi.org/10.1002/anie.201611072>.
- Højsgaard, S., Halekoh, U., 2016. doBy: Groupwise Statistics, LSmeans, Linear Contrasts, Utilities. R Package Version 4.5-15. <https://CRAN.R-project.org/package=doBy>.
- Jacob, D., Petersen, J., Eggert, B., Alias, A., Christensen, O.B., Bouwer, L.M., Braun, A., Colette, A., Déqué, M., Georgievski, G., Georgopoulou, E., Gobiet, A., Menut, L., Nikulin, G., Haensler, A., Hempelmann, N., Jones, C., Keuler, K., Kovats, S., Kröner, N., Kotlarski, S., Kriegsmann, A., Martin, E., van Meijgaard, E., Moseley, C., Pfeifer, S., Preuschmann, S., Radermacher, C., Radtke, K., Rechid, D., Rounsevell, M., Samuelsson, P., Somot, S., Soussana, J.-F., Teichmann, C., Valentini, R., Vautard, R., Weber, B., Yiou, P., 2014. EURO-CORDEX: new high-resolution climate change projections for european impact research. *Reg. Environ. Chang.* 14, 563–578. <https://doi.org/10.1007/s10113-013-0499-2>.
- Jones, P., Kilsby, C., Harpham, C., Glenis, V., Burton, A., 2009. UK climate projections science report: projections of future daily climate for the UK from the weather generator. UK Climate Projections Science Report. University of Newcastle, London, UK.
- Jordan, A., Gathergood, N., 2015. Biodegradation of ionic liquids—a critical review. *Chem. Soc. Rev.* 44, 8200–8237. <https://doi.org/10.1039/C5CS00444F>.
- Kubo, A.-L., Kremer, L., Herrmann, S., Mitchell, S.G., Bondarenko, O.M., Kahru, A., Streb, C., 2017. Antimicrobial activity of polyoxometalate ionic liquids against clinically relevant pathogens. *ChemPlusChem* 82, 867–871. <https://doi.org/10.1002/cplu.201700251>.
- La Russa, M.F., Macchia, A., Ruffolo, S.A., De Leo, F., Barberio, M., Barone, P., Crisci, G.M., Urzi, C., 2014. Testing the antibacterial activity of doped TiO₂ for preventing biodeterioration of cultural heritage building materials. *Int. Biodeterior. Biodegradation* 96, 87–96. <https://doi.org/10.1016/j.ibiod.2014.10.002>.
- Liu, X., Koestler, R.J., Warscheid, T., Katayama, Y., Gu, J.-D., 2020. Microbial deterioration and sustainable conservation of stone monuments and buildings. *Nat. Sustain.* 1–14. <https://doi.org/10.1038/s41893-020-00602-5>.
- Lo Schiavo, S., De Leo, F., Urzi, C., 2020. Present and future perspectives for biocides and antifouling products for stone-built cultural heritage: ionic liquids as a challenging alternative. *Appl. Sci.* 10, 6568. <https://doi.org/10.3390/app10186568>.
- Luvdi, L., Mecchi, A.M., Ferretti, M., Sidoti, G., 2016. Treatments with self-cleaning products for the maintenance and conservation of stone surfaces. *Int. J. Conserv. Sci.* 7, 311–322.
- Mascalchi, M., Orsini, C., Pinna, D., Salvadori, B., Siano, S., Rimesini, C., 2020. Assessment of different methods for the removal of biofilms and lichens on gravestones of the english cemetery in Florence. *Int. Biodeterior. Biodegradation* 154, 105041. <https://doi.org/10.1016/j.ibiod.2020.105041>.
- Misra, A., Franco Castillo, I., Müller, D.P., González, C., Eyssautier-Chuine, S., Ziegler, A., de la Fuente, J.M., Mitchell, S.G., Streb, C., 2018. Polyoxometalate-ionic liquids (POM-ILs) as anticorrosion and antibacterial coatings for natural stones. *Angew. Chem. Int. Ed.* 57, 14926–14931. <https://doi.org/10.1002/anie.201809893>.
- Moreau, C., Vergès-Belmin, V., Leroux, L., Orial, G., Fronteau, G., Barbin, V., 2008. Water-repellent and biocide treatments: assessment of the potential combinations. *J. Cult. Herit.* 9, 394–400. <https://doi.org/10.1016/j.culher.2008.02.002>.
- Pereira, D., Tournier, F., Bernáldez, L., Blázquez, A.G., 2015. Petit granit: a belgian limestone used in heritage, construction and sculpture. *Episodes J. Int. Geosci.* 38, 85–90. <https://doi.org/10.18814/epiugs/2015/v38i2/003>.
- Petkovic, M., Seddon, K.R., Rebelo, L.P.N., Pereira, C.S., 2011. Ionic liquids: a pathway to environmental acceptability. *Chem. Soc. Rev.* 40, 1383–1403. <https://doi.org/10.1039/C004968A>.
- Pfendler, S., Alaoui-Sossé, B., Alaoui-Sossé, L., Bousta, F., Aleya, L., 2018. Effects of UV-C radiation on *Chlorella vulgaris*, a biofilm-forming alga. *J. Appl. Phycol.* 30, 1607–1616. <https://doi.org/10.1007/s10811-017-1380-3>.
- Pinna, D., 2021. Microbial growth and its effects on inorganic heritage materials. *Microorganisms in the Deterioration and Preservation of Cultural Heritage*. Springer, Neuchâtel, Switzerland, p. 364.
- R Core Team, 2014. R Foundation for Statistical Computing. <http://www.R-project.org/>.
- Rajkowska, K., Koziróg, A., Otlewska, A., Piotrowska, M., Adrián-Blasco, E., Franco-Castillo, I., Mitchell, S.G., 2020. Antifungal activity of polyoxometalate-ionic liquids on historical brick. *Molecules* 25, 5663. <https://doi.org/10.3390/molecules25235663>.
- Reyes-Estebanez, M., Ortega-Morales, B.O., Chan-Bacab, M., Granados-Echegoyen, C., Camacho-Chab, J.C., Pereañez-Sacarias, J.E., Gaylarde, C., 2018. Antimicrobial engineered nanoparticles in the built cultural heritage context and their ecotoxicological impact on animals and plants: a brief review. *Heritage Sci.* 6, 1–11. <https://doi.org/10.1186/s40494-018-0219-9>.
- Romani, M., Adouane, E., Carrion, C., Vecklerl, C., Boeuf, D., Fernandez, F., Lefèvre, M., Intertaglia, L., Rodrigues, A.M.S., Lebaron, P., Lami, R., 2021. Diversity and activities of pioneer bacteria, algae, and fungi colonizing ceramic roof tiles during the first year of outdoor exposure. *Int. Biodeterior. Biodegradation* 162, 105230. <https://doi.org/10.1016/j.ibiod.2021.105230>.
- Romani, M., Warscheid, T., Nicole, L., Marcon, L., Di Martino, P., Suzuki, M.T., Lebaron, P., Lami, R., 2022. Current and future chemical treatments to fight biodeterioration of outdoor building materials and associated biofilms: moving away from ecotoxic and towards efficient, sustainable solutions. *Sci. Total Environ.* 802, 149846. <https://doi.org/10.1016/j.scitotenv.2021.149846>.
- Ruffolo, S.A., De Leo, F., Ricca, M., Arcudi, A., Silvestri, C., Bruno, L., Urzi, C., La Russa, M.F., 2017. Medium-term in situ experiment by using organic biocides and titanium dioxide for the mitigation of microbial colonization on stone surfaces. *Int. Biodeterior. Biodegrad.* 123, 17–26. <https://doi.org/10.1016/j.ibiod.2017.05.016>.
- Santo, A.P., Cuzman, O.A., Petrocchi, D., Pinna, D., Salvatici, T., Perito, B., 2021. Black on white: microbial growth darkens the external marble of Florence Cathedral. *Appl. Sci.* 11, 6163. <https://doi.org/10.3390/app11136163>.

- Sasso, S., Miller, A.Z., Rogerio-Candelera, M.A., Cubero, B., Coutinho, M.L., Scrano, L., Bufo, S.A., 2016. Potential of natural biocides for biocontrolling phototrophic colonization on limestone. *Int. Biodeterior. Biodegradation* 107, 102–110. <https://doi.org/10.1016/j.ibiod.2015.11.017>.
- Shilova, O.A., Vlasov, D.Y., Zelenskaya, M.S., Ryabusheva, Y.V., Khamova, T.V., Glebova, I.B., Sinelnikov, A.A., Marugin, A.M., Frank-Kamenetskaya, O.V., 2020. Sol-gel derived TiO₂ and epoxy-titanate protective coatings: structure, property, fungicidal activity and biomineralization effects. *Processes and Phenomena on the Boundary Between Biogenic and Abiogenic Nature*. Springer, pp. 619–638 https://doi.org/10.1007/978-3-030-21614-6_33 ISSN: 21938571.
- Shilova, O.A., Vlasov, D.Y., Khamova, T.V., Zelenskaya, M.S., Frank-Kamenetskaya, O.V., 2022. Microbiologically induced deterioration and protection of outdoor stone monuments. *Biodegradation and Biodeterioration at the Nanoscale*. Elsevier, pp. 339–367 <https://doi.org/10.1016/B978-0-12-823970-4.00015-4>.
- Smarsly, B., Kaper, H., 2005. Liquid inorganic–organic nanocomposites: novel electrolytes and ferrofluids. *Angew. Chem. Int. Ed.* 44, 3809–3811. <https://doi.org/10.1002/anie.200500690>.
- Speranza, M., Wierzbos, J., De Los Rios, A., Perez-Ortega, S., Souza-Egipsy, V., Ascaso, C., 2012. Towards a more realistic picture of in situ biocide actions: combining physiological and microscopy techniques. *Sci. Total Environ.* 439, 114–122. <https://doi.org/10.1016/j.scitotenv.2012.09.040>.
- Streb, C., 2012. New trends in polyoxometalate photoredox chemistry: from photosensitisation to water oxidation catalysis. *Dalton Trans.* 41, 1651–1659. <https://doi.org/10.1039/C1DT11220A>.
- Urzi, C., De Leo, F., Bruno, L., Pangallo, D., Krakova, L., 2014. *New species description, biomineralization processes and biocleaning applications of Roman catacombs-living bacteria. The Conservation of Subterranean Cultural Heritage*. CRC Press, pp. 65–72.
- Vlasov, D.Yu., Parfenov, V.A., Zelenskaya, M.S., Plotkina, Y.V., Geludova, V.M., Frank-Kamenetskaya, O.V., Marugin, A.M., 2019. Methods of monument protection from damage and their performance. In: Frank-Kamenetskaya, O.V., Rytikova, V.V., Vlasov, D.Yu (Eds.), *The Effect of the Environment on Saint Petersburg's Cultural Heritage: Results of Monitoring the Historical Necropolis Monuments, Geoheritage, Geoparks and Geotourism*. Springer International Publishing, Cham, pp. 161–178 https://doi.org/10.1007/978-3-319-79072-5_7.
- Warscheid, Th., Braams, J., 2000. Biodeterioration of stone: a review. *Int. Biodeterior. Biodegrad.* 46, 343–368. [https://doi.org/10.1016/S0964-8305\(00\)00109-8](https://doi.org/10.1016/S0964-8305(00)00109-8).
- Warscheid, T., Leisen, H., 2011. *Microbiological studies on stone deterioration and development of conservation measures at Angkor Wat. Biocolonization of Stone: Control and Preventive Methods, Proceedings from the MCI Workshop Series. Presented at the MCI Workshop Series*. Smithsonian Institution Scholarly Press, Washington, pp. 1–18.
- Wasserscheid, P., Keim, W., 2000. Ionic liquids—new “solutions” for transition metal catalysis. *Angew. Chem. Int. Ed.* 39, 3772–3789. [https://doi.org/10.1002/1521-3773\(20001103\)39:21<3772::AID-ANIE3772>3.0.CO;2-5](https://doi.org/10.1002/1521-3773(20001103)39:21<3772::AID-ANIE3772>3.0.CO;2-5).
- Wickham, H., 2009. *ggplot2: Elegant Graphics for Data Analysis*. <http://ggplot2.tidyverse.org> <https://github.com/tidyverse/ggplot2>.
- Wickham, H., 2016. *readxl: Read Excel Files. R Package Version 0.1.1*. <https://CRAN.R-project.org/package=readxl>.
- Zarzuela, R., Carbú, M., Gil, M.L.A., Cantoral, J.M., Mosquera, M.J., 2016. CuO/SiO₂ nanocomposites: a multifunctional coating for application on building stone. *Mater. Des.* 114, 364–372. <https://doi.org/10.1016/j.matdes.2016.11.009>.